Topological Aspects of Conformational Coupling in 8,8-Dimethyl-1,4-diheterospiro[4.5]decanes: A Molecular Mechanics Study

P. Iratcabal*,† and D. Liotard‡

Contribution from the Laboratoire de Chimie Organique Physique and the Laboratoire de Chimie Structurale, Centre Universitaire de Recherche Scientifique, Avenue de l'Université, 64000 Pau, France. *Received May 15, 1987*

Abstract: We present the conformational analysis of 8,8-dimethyl-1,4-diheterospiro[4.5]decanes based on molecular mechanics calculations. To model the dynamic behavior of these compounds a topological approach is taken. A general strategy to the investigation of high dimensional potential energy surfaces is developed. A mathematical formulation of the concept of conformational coupling is proposed in terms of curvature properties and bifurcations. Clear evidence is obtained for correlated movements of the two rings in these molecules. Several flipping schemes are suggested which rationalize the experimental data.

As a part of the vast amount of DNMR work expended on conformational isomerization in cyclohexyl systems[1] a few studies have been concerned with spiro compounds containing heterocyclic five-membered rings.[2,3] A remarkable result in this series is that the barrier to inversion of the cyclohexane ring shows an appreciable dependence on heteroatom(s). We observed ourselves that replacing oxygen atoms by sulfur led to an increase of ca. 1.4 kcal·mol^{-1} in the barrier of 8,8-dimethyl-1,4-diheterospiro[4.5]-decanes (Figure 1).

Various strategies can be adopted for the study of the relevant potential energy surfaces depending on the purpose to be achieved. If the conformational coupling between rings A and B is to be understood then the detailed knowledge of the potential energy as a function of the internal degrees of freedom of the two rings is required. If the goal is only the knowledge of gross information compatible with the available experimental data then only the degrees of freedom of ring A are to be investigated. A common tool would be to "switch off" the degrees of freedom corresponding to the *gem*-dimethyl and heterocyclic moieties by constraining them to some predetermined geometry (cross-section approach). However, the reaction paths obtained in this way have a poor chemical significance since different cross-sections can produce different paths. Moreover, no actual critical point of the surface can be reached this way. A better strategy would be to relax the geometry of the *gem*-dimethyl and ring B fragments for each trial geometry of ring A. We call this procedure the partial minimization approach. It allows us to reach the critical points belonging to some non-ramifying subset (one connected component) of the potential surface. For example, the deformations of the central ring A in 9,9-dimethyl-1,5-diheterospiro[5.5]undecanes occur without significant relaxation of the geometry of ring B.[4] Therefore, a three-dimensional (3-D) subset of the entire surface can be chosen in which all conformational changes are sufficient to rationalize the experimental data. However, in the case of flat profiles (such as in pseudorotating heterocyclic five-membered rings[5]), this procedure does not guarantee the coverage of a one-piece non-ramifying subset of the potential surface even if the results are topologically coherent.[4,6,7]

After two accounts dealing with systems containing fairly "rigid" spiro-substituents,[4,7] the possibility of increased "flexibility" of this substituent is now pursued. We report in the present paper a computational analysis of the potential energy hypersurface of **1** and **2** (Figure 1) by molecular mechanics calculations.[8]

As a result of the mobility of ring B some correlated movements can occur, i.e., both rings A and B may participate in a composite isomerization process. Apart from the reproduction of the experimental barriers this report provides an answer to the mechanistic questions posed by these compounds: (i) is the flip of the spiranic fragment involved in the rate-determining step of the transformation, (ii) can the potential energy hypersurface be

† Laboratoire de Chimie Organique Physique.
‡ Laboratoire de Chimie Structurale.

(1) (a) Johnson, C. S. *Adv. Magn. Reson.* **1965**, 33. (b) Binsch, G. *Top. Stereochem.* **1968**, *3*, 97. (c) Sutherland, I. O. *Ann. Rep. NMR Spectrosc.* **1971**, *4*, 71. (d) Anet, F. A. L. *Top. Curr. Chem.* **1974**, *45*, 169. (e) Anderson, E. J. *Top. Curr. Chem.* **1974**, *45*, 139. (f) Anet, F. A. L.; Anet, R. *Dynamic Nuclear Magnetic Resonance Spectroscopy*; Jackman, L. M., Cotton, F. A., Eds.; Academic: New York, 1975; 543. (g) Mann, B. E. *Prog. NMR Spectrosc.* **1977**, *11*, 95. (h) Sandstrom, J. *Dynamic NMR Spectroscopy*, Academic: New York, 1982.

(2) (a) Murray, R. W.; Kaplan, M. L. *Tetrahedron* **1967**, *23*, 1575. (b) Friebolin, H.; Schmid, H. G.; Kabuss, S.; Faist, W. *Org. Magn. Res.* **1969**, *1*, 147. (c) Granger, R.; Robbe, Y.; Chapat, J. P.; Bitoun, J.; Terol, A.; Guerret, P. *Bull. Soc. Chim. Fr.* **1975**, *5-6*, 1201.

(3) Iratcabal, P.; Grenier-Loustalot, M. F.; Lichanot, A.; Metras, F. *Org. Magn. Reson.* **1980**, *14*, 451.

(4) Iratcabal, P.; Liotard, D. *J. Comput. Chem.* **1986**, *7*, 482.

(5) (a) Dauben, W. G.; Pitzer, K. S. In *Steric Effects in Organic Chemistry*; Newman, M. S., Ed.; Wiley: New York, 1956; Chapter 1. (b) Eliel, E. L.; Allinger, N. L.; Angyal, S. J.; Morrison, G. A. *Conformational Analysis*; Interscience: New York, 1965; p 200. (c) Hanack, M. *Conformation Theory*; Academic: New York, 1965; p 72. (d) Romers, C.; Altona, C.; Buys, H. R.; Havinga, E. *Top. Stereochem.* **1969**, *4*, 39. (e) Laane, J. In *Vibrational Spectra and Structure*; Durig, J. R., Ed.; Marcel Dekker: New York, 1972; Vol. 1. (f) Fuchs, B. *Top. Stereochem.* **1978**, *10*, 1. (g) Legon, A. C. *Chem. Rev.* **1980**, *80*, 231.

(6) (a) Morse, M. Calculus of Variation in the Large, American Mathematical Society Colloquium Publications, 1934; Vol. 18. (b) Munkres, J. *Elementary Differential Topology Annals of Mathematical Studies*, Princeton University Press: Princeton, 1963; Vol. 54. (c) Spanier, E. H. *Algebraïc Topology*; McGraw Hill: New York, 1966. (d) Morse, M.; Cairns, S. S.; *Critical Point Theory in Global Analysis and Differential Topology*; Academic: New York, 1969. (e) Milnor, J. *Morse Theory, Annals of Mathematical Studies*; Princeton University Press: Princeton, 1973; Vol. 51. (f) Mezey, P. G. *Prog. Theor. Org. Chem.* **1977**, *2*, 127. (g) Mezey, P. G. In *Chemical Applications of Topology and Graph Theory*; King, R. B. Ed.; Elsevier: Amsterdam, 1983; p 75. (h) Peterson, M. R.; Csizmadia, I. G.; Sharpe, R. W. *J. Mol. Struct. Theochem.* **1983**, *94*, 127. (i) Csizmadia, I. G. In *Symmetries and properties of non rigid molecules*; Maruani, J., Serre, J., Eds.; Elsevier: New York, 1983. (j) Liotard, D. In *Symmetries and properties of non rigid molecules*; Maruani, J., Serre, J., Eds.; Elsevier: New York, 1983. (k) Cardy, H.; Liotard, D.; Dargelos, A.; Poquet, E. *Chem. Phys.* **1983**, *77*, 287.

(7) Iratcabal, P.; Liotard, D.; Grenier-Loustalot, M. F.; Lichanot, A. *J. Mol. Struct. Theochem.* **1985**, *124*, 51.

(8) (a) Westheimer, F. H. In *Steric Effects in Organic Chemistry*; Newman, M. S., Ed.; Wiley: New York, 1956; Chapter 12. (b) Williams, J. E.; Stang, P. J.; Schleyer, P. v. R. *Annu. Rev. Phys. Chem.* **1968**, *19*, 531. (c) Engler, E. M.; Andose, J. D.; Schleyer, P. v. R. *J. Am. Chem. Soc.* **1975**, *95*, 8005. (d) Altona, C.; Faber, D. H. *Top. Curr. Chem.* **1974**, *45*, 1. (e) Simonetta, M. *Acc. Chem. Res.* **1974**, *7*, 345. (f) Ermer, O. *Struct. Bonding* **1976**, *27*, 161. (g) Allinger, N. L. *Adv. Phys. Org. Chem.* **1976**, *13*, 1. (h) Niketic, S. R.; Rasmussen, K. *The Consistent Force Field*; Springer: Berlin, 1977. (i) Hursthouse, M. B.; Moss, G. P.; Sales, K. D. *Annu. Rep. Sect. B. Org. Chem.* **1978**, *75*, 23. (j) Kitaigorodsky, A. I. *Chem. Soc. Rev.* **1978**, *7*, 133. (k) Boyd, D. B.; Lipkowitz, K. B. *J. Chem. Educ.* **1982**, *59*, 269. (l) Osawa, E.; Musso, H. *Top. Stereochem.* **1982**, *13*, 117. (m) Burkert, U.; Allinger, N. L. *Molecular Mechanics*; ACS Monograph, 1982; No. 177. (n) Dashevskii, V. G. *Konformatzionnoi Analyz Organicheskih Molekul. Chimia*, Moscow, 1982. (o) Osawa, E.; Musso, H. *Angew. Chem., Int. Ed. Engl.* **1983**, *22*, 1. (p) Lomas, J. S. *Actualité Chimique* **1986**, *5*, 7.

0002-7863/88/1510-4919$01.50/0

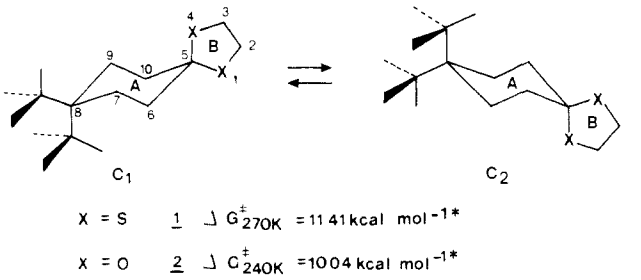

Figure 1. Conformational equilibrium in 8,8-dimethyl-1,4-diheterospiro[4.5]decanes. The asterisk shows activation parameters derived from a refinement of previous results[3] (experimental and computed bandshapes of the ^{13}C spectra in the methyl region are available as supplementary material).

reduced to a 3-D subset containing the exclusive conformational information relevant to ring A and designed for a visual representation as done in?[4] We shall take here a further opportunity to evidence the usefulness of the interplay between topology[4,6,7] and conformational analysis in high-dimensional stereochemical problems.

In section I we focus the investigation on the treatment of the conformational coupling. We begin with the mathematical aspects of the problem, in terms of critical points count and index (i.e., the number of negative eigenvalues of the Hessian matrix—the Hessian is the matrix of second derivatives which dictates the curvatures of the surface in the neighborhood of a critical point; the index is required to characterize a critical point as a minimum (index = 0), a transition state (index = 1), or another (index > 1)). Next, we examine the critical points and indices of the potential surface of models for free rings A and B: 1,1-dimethylcyclohexane for A, 1,3-dioxolane and 1,3-dithiolane for B. Finally, we investigate the entire set of critical points of the potential surfaces of **1** and **2**. During optimization, no constraints were imposed on the up to 96 degrees of freedom of these molecules. A detailed analysis of some typical interconversion pathways is presented. Such a protocol provides the most reliable information about the concertedness of the processes but it is faced with the intrinsic complexity of the interconversion web. Actually, the network lies in a 5-D subspace and no simple graphical representation can be given.

In section II, we derive from the entire hypersurface the gross chemical information in terms of a 3-D effective potential surface, simpler to analyze and visualize through a graph. The procedure consists of a smoothing of adjacent critical points when not essential in the interpretation of the DNMR results: the critical points are to be removed by pairs according to energetic and geometric criteria thus leading to a smoothed surface embedding a 3-D subset where the remaining critical points lie.

The Morse theory[4,6c-g,7] is extensively used throughout this study. The Morse inequalities interrelate the number (N_k) of critical points of index k with the Betti numbers of rank k (R_k). The Betti numbers depend only on the topological features of the space underlying the potential function (and not on the potential surface itself). For the Cartesian space, they are

$$R_0 = 1 \qquad R_k = 0 \ (k > 0)$$

For any smooth function with no degenerate critical points (i.e., no zero eigenvalue of the Hessian), one has

$$N_k \geq R_k \tag{1}$$

$$N_k - N_{k-1} + \ldots + (-1)^k N_0 \geq R_k - R_{k-1} + \ldots + (-1)^k R_0 \tag{2}$$

and the equality holds in eq 2 when k reaches the dimensionality of the space. These relations can be used as diagnostics for completeness of the set of critical points at any stage of a numerical prospection either for the entire surface or in a partial minimization approach. In building up the effective potential surface, the Morse theory provides also a decisive answer to decide whether a given pair of critical points can be removed or not.

I. Topological Properties of Potential Surfaces and Conformational Coupling

1. Some Mathematical Aspects of Coupling: Bifurcation of Surface. Let us suppose that for some chemical purposes, the energy of a molecule is conveniently partitioned as a sum of three terms depending on the nuclear coordinates

$$E_T(x) = E_A(x_A) + E_B(x_B) + \lambda E_p(x_A, x_B) \tag{3}$$

where E_A and E_B are the contributions from the fragments A and B, E_p is the coupling term between the fragments, and λ is a formal perturbation parameter evolving from 0 to 1.

Coupling effects are often discussed on energetic grounds,[9] but topological aspects are usually disregarded in chemistry.

Let Y_A and Y_B be two critical points of E_A and E_B, respectively. Usually the point $Y = (Y_A, Y_B)$ is not a critical point of E_T. However, under the very mild assumption that both E_A and E_B are Morse functions, the Hessian in the neighborhood of Y can be written as

$$H = H_0 + P(\lambda)$$

where H_0 is the (nondegenerated) block-diagonal Hessian of the unperturbed function $E_A + E_B$ and P is a perturbation matrix depending on λ. Then it follows from the chain rule (ref 10a, section 1) that for a small enough value of λ ($\lambda < \lambda_0$), the Hessian H remains continuously nondegenerated (no vanishing eigenvalue) and there exists one and only one critical point $Z = (Z_A, Z_B)$ of E_T which converges to Y as λ vanishes.

Therefore, for a small enough value of λ, the global topology of E_T does not differ from that of $E_A + E_B$. More precisely

$$n_T = n_A \cdot n_B \tag{4}$$

where n_A, n_B, n_T are the numbers of critical points of E_A, E_B, E_T, respectively, and

$$I_T(Z) = I_A(Y_A) + I_B(Y_B) \tag{5}$$

where I_T is the index of the perturbed critical point Z and $I_A + I_B$ is the index of the unperturbed one Y.

Obviously, coupling effects on topological features such as critical point and index or reaction paths network are actually dictated by second-order properties of E_P with respect to those of $E_A + E_B$ and not by energetics only. For weakly coupled cases (i.e., $\lambda < \lambda_0$), relations 4 and 5 are valid and enlarge to any kind of partitioned molecular system the "kappa rule" previously proposed for internal rotators.[11] In such a case, the knowledge of E_A and E_B is sufficient to predict and classify the critical points of E_T and the associated reaction paths network.

As soon as the perturbation parameter λ goes beyond the bifurcation threshold λ_0, the location, indices, and number of critical points can evolve abruptly. However, global analysis overcomes these local discontinuities and Morse theory does apply on both sides of the threshold λ_0. Various bifurcations can be observed and classified according to Catastrophe Theory.[10] For the simplest case (the fold) where only one eigenvalue of the Hessian H vanishes at λ_0, a couple of adjacent critical points differing by one in indices is created (or anihilated). Most of the other cases (unless symmetrically constrained) can be studied by the method of contraction which proceeds by "pulling together" adjacent critical points in fold catastrophes (ref 10a, section 7). If one allows a "temporary" distortion of the nonrigid symmetry of a potential function, the method of contraction provides a natural selection rule governing the modification of potential hypersurfaces as recently illustrated in chemistry.[12]

Anyway, as soon as the coupling is strong, some bifurcations are encountered and a complete search for the critical points of E_T cannot be avoided.

(9) Tavernier, D.; Anteunis, M.; Hosten, N. *Tetrahedron Lett.* **1973**, *1*, 75.

(10) (a) Gilmore, R. *Catastrophe Theory for Scientists and Engineers*; Wiley: New York, 1981. (b) Zeeman, E. C. *Catastrophe Theory*; Addison-Wiley: New York, 1977.

(11) Csizmadia, I. G. *J. Mol. Struct. Theochem.* **1986**, *138*, 1.

(12) Angyan, J. G.; Daudel, R.; Kucsman, A.; Csizmadia, I. G. *Chem. Phys. Lett.* **1987**, *136:1*, 1.

Table I. Torsional Features, Energies, and Indices for Nonsymmetrically Related Critical Points of 1,1-Dimethylcyclohexane

conformation	dihedral angles[a] 5-6-7-8	6-7-8-9	7-8-9-10	8-9-10-5	9-10-5-6	10-5-6-7	strain energy, kcal·mol^{-1}	index
C (C_s)	55.4	-52.6	52.6	-55.4	56.0	-56.0	4.55	0
TB1 (C_2)	64.4	-31.0	-31.0	64.4	-30.6	-30.6	9.17	0
TB2	42.1	15.8	-57.7	38.5	20.8	-62.1	10.17	0
B1 (C_s)	0.3	45.1	-45.1	-0.3	46.9	-46.9	13.52	1
B2	55.1	-3.1	-49.2	49.2	4.0	-55.4	10.59	1
HC1	-16.0	53.9	-65.1	36.7	3.8	-14.2	14.67	1
HB1 (C_s)	28.3	7.8	-7.8	-28.3	64.4	-64.4	15.72	2
HB2 (C_s)	-25.0	59.8	-59.8	25.0	12.1	-12.1	14.70	2
HB3	65.5	-29.6	-5.6	5.2	30.0	-64.8	15.13	1
HB4	10.2	19.1	-57.0	65.2	-33.3	-2.9	15.88	2
P (C_{2v})	all dihedral angles equal to zero						30.27	3

[a] Atom numbering as defined in **1** and **2** (Figure 1).

Table II. Torsional Features, Energies, and Indices for Nonsymmetrically Related Critical Points of 1,3-Dithiolane and 1,3-Dioxolane

compounds	conformation	dihedral angles 1-2-3-4	2-3-4-5	3-4-5-1	4-5-1-2	5-1-2-3	strain energy, kcal·mol^{-1}	index
1,3-dithiolane	HC1 (C_2)	51.9	-38.8	12.4	12.4	-38.8	0.37	1
	HC2	43.3	-14.8	-18.8	39.5	-50.0	0.03	0
	E (C_s)	0.0	29.0	-47.2	47.2	-29.0	1.19	1
	P (C_{2v})	all dihedral angles equal to zero					5.56	2
1,3-dioxolane	HC1 (C_2)	38.9	-30.9	12.7	12.7	-30.9	5.55	1
	E (C_s)	0.0	23.6	-39.9	39.9	-23.6	5.19	0
	P (C_{2v})	all dihedral angles equal to zero					8.34	2

2. The Potential Energy Surface of Free Rings A and B. From the preceding mathematical considerations it can be easily deduced that the knowledge of the critical points of the potential surface of free rings A and B is of fundamental importance for the discussion on possible concerted movements in **1** and **2**. 1,1-Dimethylcyclohexane and 1,3-dihetero five-membered rings serve as models in this study.

(a) Ring A (Table I). For the *gem*-dimethyl group a minimum energy conformation in which the hydrogen atoms adopt a staggered position is maintained throughout the entire surface. Therefore, the contribution of this unit to the global index of the system is zero.

Like in cyclohexane the chair is found to be the most stable conformation, in agreement with both experimental[13] and other MM[14] investigations.

1,1-Dimethylcyclohexane can flip in a manner similar to the familiar inversion of cyclohexane.[4,7,8g,15] Six conformations (namely TB1, TB2, and their symmetrically related structures) correspond to twist-boat minima lying 4–6 kcal above the chairs. The isomerization paths linking the chair and the twist-boat family go through eight possible routes. Four of them involve half-chair type transition states (HC1); the others proceed via half-boat forms of higher energy (HB3). The calculated barriers, respectively 10.12 and 10.58 kcal for the HC1 and HB3 processes, are in agreement with experimental data.[16] Connecting the twist-boat conformations through a pseudorotational circuit we find six boat conformations with index 1. Finally, eight second-order critical points (HB1, HB2, HB4, plus their enantiomeric and inverted structures) and the planar form with index 3 lie also on the potential surface.

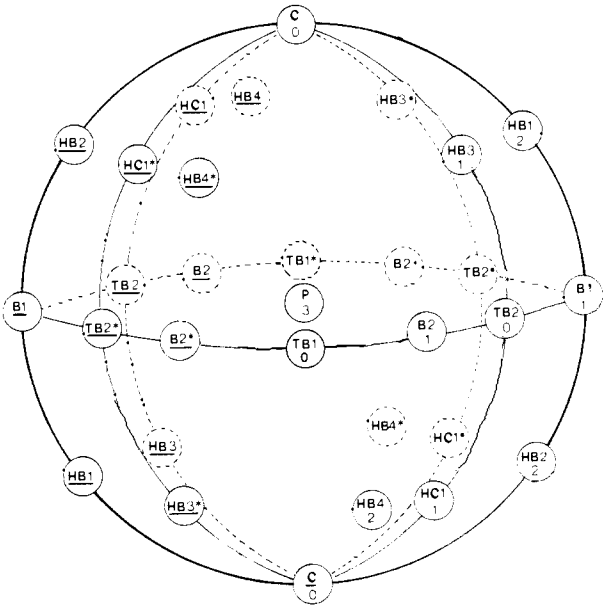

Figure 2. Topological graph of the potential energy of 1,1-dimethylcyclohexane with critical points and reaction paths network. The index of each nonsymmetrically related critical point (generator) is given below its label. The C_{2v} symmetry operation "*" acts as the mirror plane C-P-B1, the operation "—" as the inversion center *P* (see Appendix for details).

As for cyclohexane,[4,15c,n,17] the whole set of critical points belong to a one-piece manifold spanned by the three "out-of-plane" motions. The Morse theory is satisfied in this manifold which provides not only a natural graph for the reaction paths network (Figure 2) but also a topologically reliable picture of the location of each critical point and indices. According to these results, the contribution of ring A to the global dimensionality of the problem in **1** and **2** is 3.

(13) Geise, H. J.; Mijlhoff, F. C.; Altona, C. *J. Mol. Struct.* **1972**, *13*, 211.
(14) (a) Altona, C.; Sundaralingham, M. *Tetrahedron* **1970**, *26*, 925. (b) Osawa, E.; Collins, J. B.; Schleyer, P. v. R. *Tetrahedron* **1977**, *33*, 2667.
(15) (a) Hendrikson, J. B. *J. Am. Chem. Soc.* **1961**, *83*, 4537. (b) Hendrikson, J. B. *J. Am. Chem. Soc.* **1967**, *89*, 7036. (c) Hendrikson, J. B. *J. Am. Chem. Soc.* **1967**, *89*, 7047. (d) Wiberg, K. B.; Boyd, R. H. *J. Am. Chem. Soc.* **1972**, *94*, 8426. (e) Ermer, O. *Tetrahedron* **1975**, *31*, 1849. (f) Van de Graaf, B.; Baas, J. M. A.; Van Veen, A. *Recl. J. R. Neth. Chem. Soc.* **1980**, *99*, 175. (g) Bucourt, R.; Hainaut, D. *Bull. Soc. Chim. Fr.* **1967**, 4563. (h) Bucourt, R. *Top. Stereochem.* **1974**, *8*, 160. (i) Allinger, N. L.; Miller, M. A.; Van Catledge, F. A.; Hirsch, J. A. *J. Am. Chem. Soc.* **1967**, *89*, 4345. (j) Allinger, N. L.; Hirsch, J. A.; Miller, M. A.; Tyminski, I. J.; Van Catledge, F. A. *J. Am. Chem. Soc.* **1968**, *90*, 1199. (k) Pickett, H. M.; Strauss, H. L. *J. Am. Chem. Soc.* **1970**, *92*, 7281. (l) Schmid, H. G.; Jaeschke, A.; Friebolin, H.; Kabuss, J.; Mecke, R. *Org. Magn. Reson.* **1969**, *1*, 163. (m) Hilderbrandt, R. L. *Comput. Chem.* **1977**, *1*, 179. (n) Dashevskii, V. G.; Verkhivker, G. M.; Kuz'min, V. E. *Dokl. Phys. Chem.* **1985**, *281*:2, 238. (o) Bixon, M.; Lifson, S. *Tetrahedron* **1967**, *23*, 769.
(16) (a) Friebolin, H.; Schmid, H. G.; Kabuss, S.; Faisst, W. *Org. Magn. Reson.* **1969**, *1*, 147. (b) Dalling, D. K.; Grant, D. M.; Johnson, L. F. *J. Am. Chem. Soc.* **1971**, *93*, 3678.
(17) Cremer, D.; Pople, J. A. *J. Am. Chem. Soc.* **1975**, *97*, 1354.

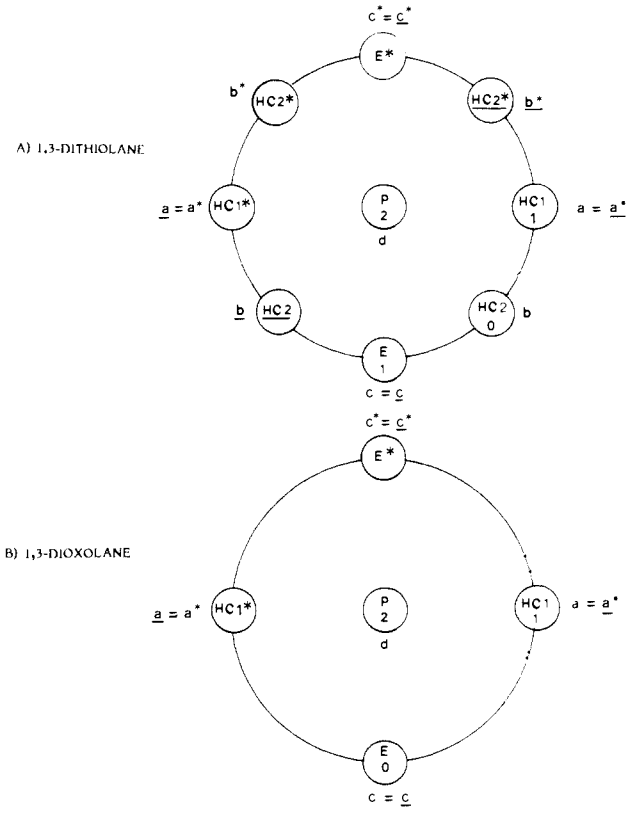

Figure 3. Topological graphs of heterocyclic five-membered rings with critical points, indices, and reaction paths network. Notations as in Figure 2 and appendix. The symmetry operation "*" acts as an inversion, the operation "—" as the vertical axis of symmetry. The small letters label the conformations of ring B in **1** and **2**, thus avoiding confusion with six-membered-ring labels in these molecules.

(b) Rings B. The number of critical points is strongly dependent on the nature of the ring but the planar form is always the highest one in energy and of index 2 (Table II). Therefore, the critical points belong to the manifold spanned by the two "out-of-plane" motions only.[5e,17,18] In the corresponding two-dimensional image, the interconversion network is given by a circle centered on the planar form (Figure 3[19]). This graph reflects the C_{2v} symmetry of the nonrigid molecule: the horizontal radial lines represent C_2 conformations (half-chair form HC) while C_s structures lie on the vertical radial lines (envelope E).

As compared with cyclopentane itself, for which 10 half-chairs (minima) and 10 envelopes (transition states) are met along the pseudorotational circuit, 1,3-dithiolane is a strongly restricted pseudorotator. Only four minima, intermediate between half-chair and envelope in shape (HC2), are interspersed with four transition states of C_2 or C_s symmetry (Figure 3A). Two different barriers of pseudorotation are possible. The lowest energy pathways involve a C_2 transition state (calculated barrier: 0.34 kcal), the alternative pathways being higher by 0.82 kcal.

In comparison with 1,3-dithiolane, the conformational mobility of 1,3-dioxolane is seriously altered. The pseudorotational process is a sequence of only four conformations (Figure 3B): one pair of ground-state C_s envelopes and two C_2 half-chair transition states. The calculated pseudorotational barrier (0.36 kcal) is consistent with experimental estimations[20] and other MM computations.[21]

Table III. Critical Points Counts

	$N_k(R_k)$					
compd	$N_0(1)$	$N_1(0)$	$N_2(0)$	$N_3(0)$	$N_4(0)$	$N_5(0)$
1	16	48	64	42	12	1
2	26	70	76	40	10	1

The barrier to planarity (3.15 kcal) reproduces fairly well the spectroscopic value (3.20 kcal from ref 22).

3. The Potential Surface of 1 and 2. The *gem*-dimethyl fragment, extracted from the most stable Cb(**1**) and Ca(**2**) conformations, was combined with each conceivable structure of rings A and B to form the initial geometries for unconstrained optimization. The rotation of the methyl groups in response to the deformations of the rest of the molecule does not exceed ±10°.

A total of 50 (**1**) and 60 (**2**) unique (i.e., not symmetrically related; application of the C_{2v} nonrigid symmetry operations brings the total number of distinguishable critical points to 183 (**1**) and 223 (**2**)) critical points were found (torsional features, energies, and indices for nonsymmetrically related critical points are available on request in the form of microfilm material: Tables VII and VIII, see appendix). They agree in number and indices with the invariants of the manifold (relations 1 and 2 and Table III).

According to eq 4 independent movements of the two rings would give 279 and 155 critical points for **1** and **2**, respectively. These hypothetical critical points can be classified matricially, with a row label referencing the conformation of ring A and a column label referencing the conformation of ring B. The actual critical points can in turn be displayed with such a labeling matrix as a canvas (Table IV). (The number of labels is 35 for rows and 9 for columns. Unexpected labels have appeared which are reminiscent of cyclohexane (rows 21 to 24) and cyclopentane (columns 2, 4, 6, 8 for **2**). As these labels have no counterpart with the labels of the free rings A and B no index has been assigned to them.) A critical point, when actually observed on the potential energy surface, is entered with its index I_T at the associated position of the matrix. (Some positions of the matrix are associated with several indices. These indices characterize critical points which only differ slightly in their structural features, the difference in energy being about a few calories.) It should be noted, however, that occasionally, due to large fluctuations in torsional angles, cataloging the conformations of rings A and B runs across serious difficulties.

Table IV contains a strong body of evidence suggesting that conformational coupling is operating in **2**. With respect to the model of uncoupled rings some expected critical points have vanished (relation 4). Bifurcations generally occur so that disappearance of a critical point of index n is accompanied by disappearance of a critical point with index $(n - 1)$ or $(n + 1)$ thus preserving topological coherence over the manifold. Unexpected conformational states are attained (rows 21 to 24 and columns 2, 4, 6, 8) for which the problem of assigning indices to rings A and B cannot be solved. Finally, the other point of interest is that I_T takes unexpected values at several critical points. For example relation 5 becomes inapplicable for some B1 and B1 conformations. These deviations constitute the most direct illustration of the effects of a perturbation acting primarily through nonbonded interactions.

Manifestations of the conformational coupling are also observed for **1** (see Table VI in the supplementary material). Apart from some discrepancies in the sequences of predicted–calculated indices much of the evidence derives from the disappearance of a great part of the expected critical points.

(18) (a) Kilpatrick, J.; Pitzer, K. S.; Pitzer, R. J. *J. Am. Chem. Soc.* **1947**, *69*, 2483. (b) Pitzer, K. S.; Donath, W. E. *J. Am. Chem. Soc.* **1959**, *81*, 3213. (c) Harris, D. O.; Engerholm, G. G.; Tolman, C. A.; Luntz, A. C.; Keller, R. A.; Kim, H.; Gwinn, W. D. *J. Chem. Phys.* **1969**, *50*, 2438. (d) Engerholm, G. G.; Luntz, A. C.; Gwinn, W. D.; Harris, D. O. *J. Chem. Phys.* **1969**, *50*, 2446. (e) Adams, W. J.; Geise, H. J.; Bartell, L. S. *J. Am. Chem. Soc.* **1970**, *92*, 5013. (f) Dunitz, J. D. *Tetrahedron* **1972**, *28*, 5459. (g) Dunitz, J. D.; Waser, J. *Elem. Math.* **1972**, *27*, 25. (h) Cremer, D.; Pople, J. A. *J. Am. Chem. Soc.* **1975**, *97*, 1358. (i) Herzyk, P.; Rabczemko, A. *J. Chem. Soc., Perkin Trans. II* **1983**, 213.

(19) Altona, C.; Sundaralingham, M. *J. Am. Chem. Soc.* **1972**, *94*, 8205.

(20) (a) Durig, J. R.; Wertz, D. W. *J. Chem. Phys.* **1968**, *49*, 675. (b) Greenhouse, J. A.; Strauss, H. L. *J. Chem. Phys.* **1969**, *50*, 124. (c) Baron, P. A.; Harris, D. O. *J. Mol. Spectrosc.* **1974**, *49*, 70.

(21) (a) Norskov-Lauritsen, L.; Allinger, N. L. *J. Comput. Chem.* **1984**, *5*, 326. (b) Allinger, N. L.; Chung, D. Y. *J. Am. Chem. Soc.* **1976**, *98*, 6798. (c) Shen, Q.; Mathers, T. L.; Raeker, T.; Hilderbrandt, R. L. *J. Am. Chem. Soc.* **1986**, *108*, 6888.

(22) Davidson, R.; Warsop, P. A. *J. Chem. Soc., Faraday Trans 2* **1972**, *68*, 1875.

Table IV. Labeling Matrix for **2**[a]

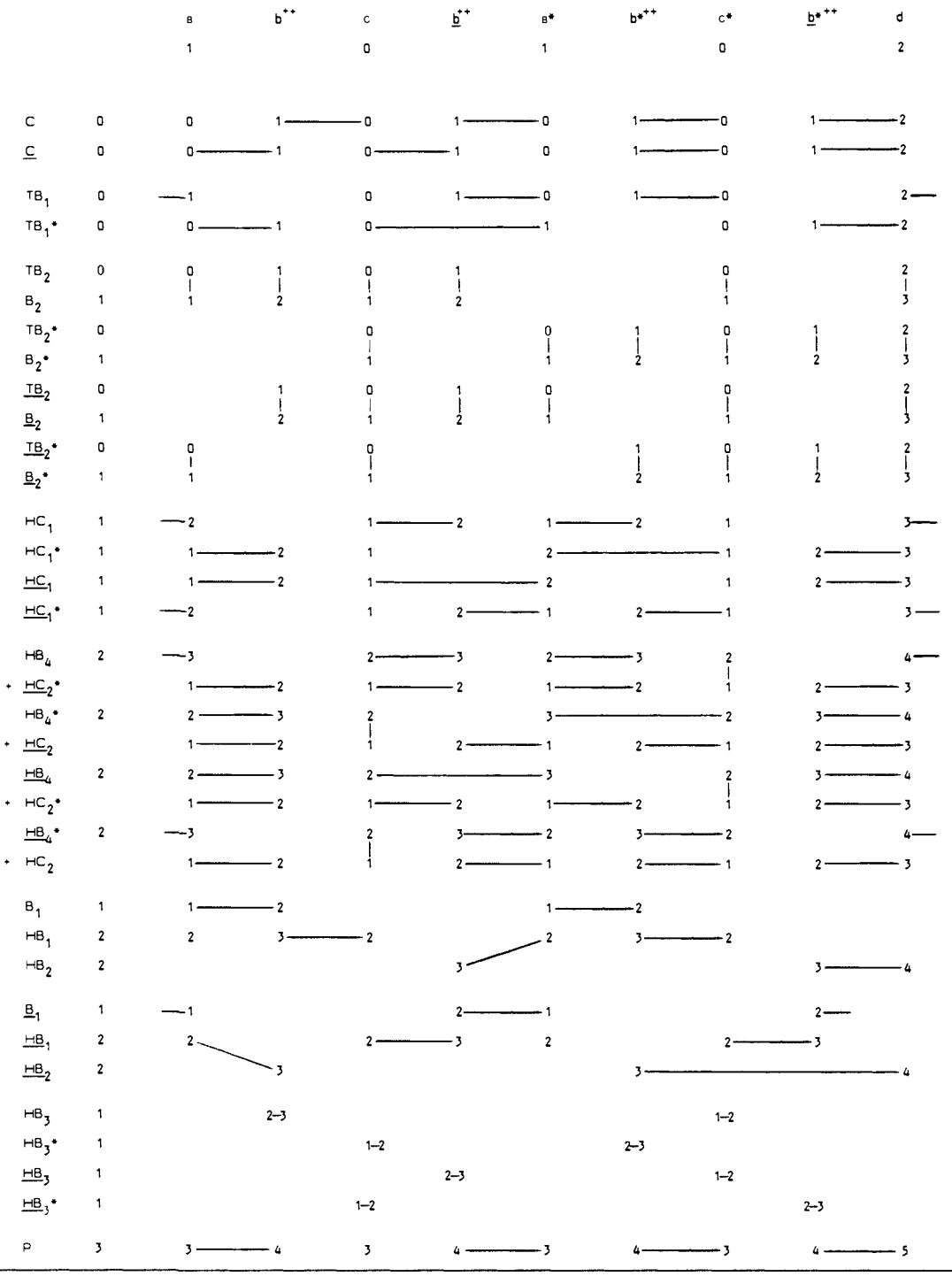

[a] Row label: conformation of ring A and index (cf. Figure 2). Column label: conformation of ring B and index (cf. Figure 3). Adjacent critical points are linked together by a straight line. Conformations marked with + are reminiscent of cyclohexane and are missing for 1,1-dimethyl cyclohexane and those with ++ are reminiscent of cyclopentane and are missing for 1,3-dioxolane.

4. The Interconversion Mechanisms. The overall agreement between calculated $\Delta H^{\ddagger}$ and experimental barriers is satisfactory, the most significant difference being a slight overestimation of the barrier in **2** (Table V and Figure 1). The decrease of the $\Delta G^{\ddagger}$ values in the sequence **1** > **2** is reproduced by computed data.

(a) Molecule 1. Exploration of the possible pathways connecting C conformations and the TB family leads to transition states in which the basic structural features of ring A closely resemble those of HC cylohexane.[7,8f,15e,f,m] Eight critical points of this type (plus their symmetrically related structures) were encountered on the potential surface. The lowest transition states are always of HC2 type. The spread between these transition states being small (~0.2 kcal), the corresponding itineraries are nearly equally populated. The pathways involving HC1 are less favorable by about 0.6 kcal·mol^{-1}. This situation is similar to that reported for 9,9-dimethyl-1,5-dithiaspiro[5.5]undecane.[4]

The C → C interconversion reaction paths network linking the lowest minima (Cb) via the lowest saddles (HC2) is shown in Figure 4. Two-ring flip mechanisms (e.g., Cb → Cb*) involve a nonlimiting saddle point (TB1a*) with C_2 symmetry, in accordance with the Stanton McIver rules.[23a] One ring flip mechanisms (e.g. Cb → Cb) have no symmetry. The entire

(23) (a) Stanton, R. E.; McIver, J. *J. Am. Chem. Soc.* **1975**, *97*, 3632. (b) Bouman, T. D.; Duncan, C. D.; Trindle, C. *Int. J. Quantum Chem.* **1977**, *11*, 399.

Table V. Calculated Barriers for C → TB Interconversion

compd	transition state involved[a]	calcd $\Delta H^{\ddagger}$,[b] kcal·mol^{-1}
1	HC2b	11.23
	HC2b*	11.28
	HC2b*	11.34
	HC2b	11.35
	HC1b*	11.82
	HC1b	11.85
	HC1b	11.99
	HC1b*	12.01
2	HC1c*	10.64
	HC1c	10.70
	HC2a	10.76
	HC2c*	10.79
	HB3c*	10.82
	HC2c	10.87
	HC2a*	10.95
	HC1a*	11.21

[a] Nonsymmetrically related structures. [b] Reactants involved: Cb for 1 and Ca for 2.

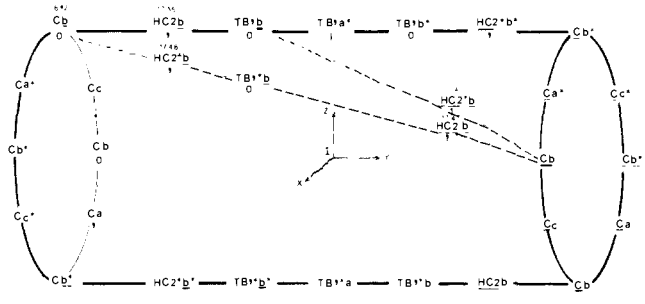

Figure 4. Network of the lowest C → C interconversion paths for 1. The network is mapped onto a cylinder for topological coherence and thus reflects the nonrigid symmetry properties of the potential. The operation "—" acts as the inversion center I, "*" as a C_2 rotation around the y axis, and the conformations with C_2 symmetry lie in the xz plane. Dotted lines represent nonsymmetrically related one-ring flip mechanisms. Typical energy values (kcal·mol^{-1}) are given above and index below the corresponding label.

network is invariant under the symmetry operations of the nonrigid C_{2v} point group in accordance with ref 23b. Two-ring flip pathways follow the absolutely lowest route (HC2b) but one-ring flip pathways require nearly the same energy (e.g., HC2*b). As a consequence, no unique answer can be afforded to the mechanistic questions raised by this compound.

(b) Molecule 2. Due to a profusion of conformational states in the TB–B region the possibilities offered to the molecule to change its conformation along the C → C isomerization process are still more numerous than in 1. Several HC and HB structures compete for the transition-state geometry (Table V) (as far as only minimum energy paths are concerned, B1a and its symmetrically related structures are likely to be dismissed on energetic grounds since they lie 0.66 kcal above the lowest transition state). Again, different two-ring flip schemes can be found which would be energetically equivalent. One-ring flip mechanisms are higher in energy by about 0.3–0.6 kcal.

II. 3-D Effective Potential Surface for 1 and 2

In a previous work[4] rationalization of the experimental data was achieved via a 3-D subset of the entire surface spanned by the three "out-of-plane" motions of the sole ring A and built up with continuous minimization of the energy within the orthogonal subset spanned by the remaining degrees of freedom.

This partial minimization approach provides topologically reliable results if and only if the orthogonal manifold is stable everywhere (i.e., no bifurcation is encountered, the orthogonal Hessian is positive-definite everywhere, and minimization of the energy always yields a unique solution). From the chemical point of view, when several 3-D subsets are available, they must essentially lead to the same information in terms of number of

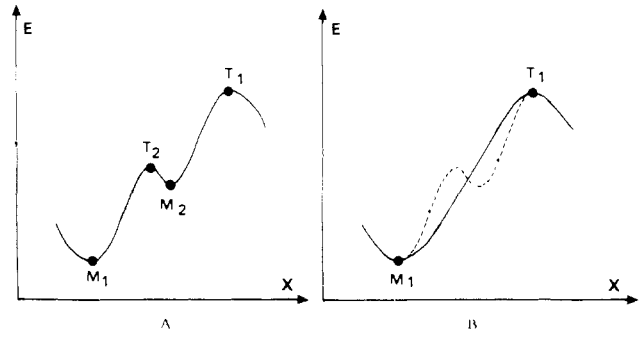

Figure 5. Energy profile for a one-dimensional trajectory connecting two minima (M_1, M_2) and two transition states (T_1, T_2): (A) before application of the "smoothing" operation and (B) after removal of the couple of critical points (M_2, T_2).

critical points and indices, notwithstanding the initially relaxed conformation of the nonexplicit molecular fragments (i.e., five-membered ring and *gem*-dimethyl group for compounds 1 and 2).

If a partial minimization approach is reliable when applied to 1 and 2 then the following properties are to be observed by inspection of the labeling matrices: (a) Each 3-D subset corresponds to a column of the matrix where one of the "reactant" and one of the "product" conformation lie. (b) The number of critical points and indices does not depend on the choice of the column among the available ones (but the energy can do). (c) Along a given row, the critical points of these columns have the same index. (d) The highest index appearing along such a column does not exceed the dimensionality of the subset (3 in our cases). (e) The Morse inequalities are satisfied within such a column.

Obviously these criteria are not satisfied by 2 and the partial minimization approach cannot be safely applied to this compound. To extract a collection of critical points carrying the most useful information, a more global strategy must be derived, insensitive to possible errors in the dispatching of the critical points in terms of labeling matrix. In building up such an "effective potential surface", chemical intuition will remain of fundamental importance, but under control of energetic, geometrical, and topological criteria. We suggest extensive use of the method of contraction as being a powerful tool in driving safely local topological modifications of surface with global consequences.

Let us begin with a 1-D example. Figure 5A displays the energy profile of a one-dimensional gradient trajectory linking two minima (M_1, M_2) and two transition states (T_1, T_2) where the measured barrier involves M_1 and T_1. If (i) M_2 and T_2 are connected by a one-step gradient trajectory, i.e., no other critical point is encountered along this trajectory, and (ii) if the energy gap between M_2 and T_2 is lower than a given threshold then these points can be pulled together without any interruption in the connectivity between M_1 and T_1 and without significant alteration of the energetic information. As a result the smoothed profile turns into a continuously ascending slope (Figure 5B). (This example can be discussed in terms of a simple geographical analogy: the small irregularities encountered along a slope by the walking mountaineer become physically undistinguishable when he flies over the region in a plane.)

Accordingly, the n-D strategy involves successive anihilation of such couples of adjacent critical points differing by one in indices. The smoothing procedure is done under topological control (i.e., the Morse inequalities must be satisfied after each anihilation) and is allowed provided that interpretation of experimental data remains unaffected. The barrier to planarity of the flexible ring B will be taken as an upper bound (4–5 kcal) for the energetic gap between adjacent critical points.

The procedure is not necessarily restricted by symmetry considerations especially when adjacent critical points do not belong to the same point group. The outcoming effective potential surface may not reflect the nonrigid symmetry of the molecular system. However, full symmetry properties can be restored on the smoothed potential surface by a trivial distortion of the remaining

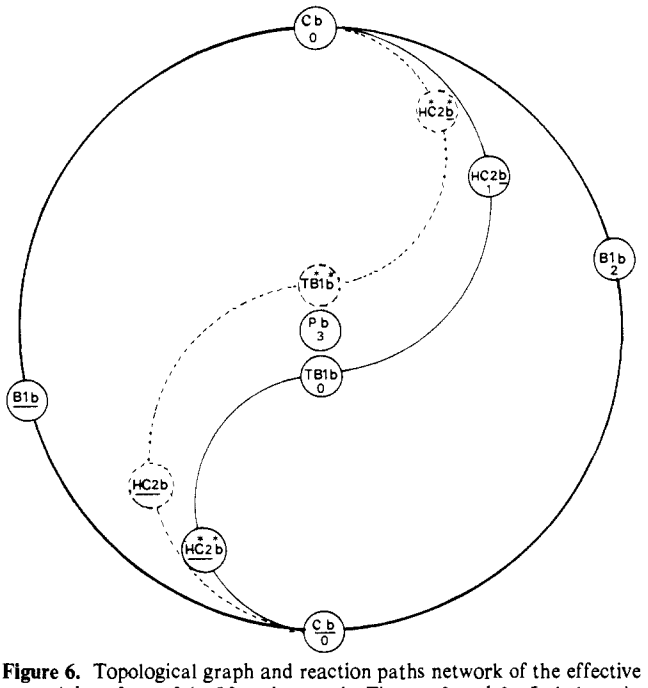

Figure 6. Topological graph and reaction paths network of the effective potential surface of **1**. Notations as in Figures 2 and 3. Labels as in Table IV.

critical points toward the correct symmetry without any subsequent change in the index. The chemical target being to keep the absolute minima and the lowest transition states, application of this strategy to **2** gives the following results (selected adjacent points are linked together in Table IV).

Rows C, C, TB1, TB1*, HC1 to HC1*, HB1, HB1, and P are contractible to one of the critical points characterized by the lowest indice, i.e., each belonging to one of the columns: a, a*, c, or c*. Rows TB2 to B2*, HB4 to B1, HB2, B1, and HB2 are erased. A critical situation is concerned with the appreciation of the geometrical proximity for ring A in HB1a* and HB2b conformations (and also in HB1a and HB2b). Actually, strictly speaking, they cannot be considered as members of the HB family but rather as distorted forms of the same B1 structure. Finally, four HB3 type critical points with index n are removed together with their close neighbors with index $(n + 1)$ (rows 31 to 34). The result is a collection of eleven critical points: four minima (Ca, Ca*, TB1c, TB1*c*), the four lowest energy transition states (HC1c*, HC1*c, HC1c*, HC1*c), two hilltops (HB1a, HB1a*), and the planar form with index three (Pc).

For compound **1** the smoothing process resembles that described previously in the case of **2**. In addition to hilltops B1b and B1b and a planar form with index three (Pb) this operation preserves the eight critical points which are of fundamental importance in the description of the interconversion paths, i.e., four minima (Cb, Cb, TB1b, TB1*b*) and four transition states (HC2b, HC2*b*, HC2b, HC2*b*).

The tests on topological coherence are conclusive for each collection of critical points and the resulting effective hypersurfaces can be mapped onto a topological sphere. The corresponding graph for compound **1** is pictured in Figure 6. Although altered by the introduction of the heterocyclic five-membered ring the symmetry properties of the cyclohexane ring can be readily visualized on the graph: (a) The reference structure of highest symmetry, the planar form (index 3), corresponds to the origin of the smoothed potential energy surface. Located at the center of the sphere it is also the inversion center for the whole conformational surface. (b) A reaction path involves two equivalent transition states (i.e., HC2b and HC2*b*) and one intermediate (TB1b) with C_2 symmetry. (c) The circle from Cb (index 0) through B1b or B1b (indices 2) to Cb (index 0) is not a reaction path. It subtends the reflexion plane converting an isomerization pathway into an enantiomeric one. B1b shows a significant flattening of ring A in comparison with the idealized structure and is located about midway between the corresponding boat and half-boat conformations of 1,1-dimethylcyclohexane (Figure 2).

III. Concluding Remarks

We have reported the analysis of the conformational hypersurface of 8,8-dimethyl-1,4-diheterospiro[4.5]decanes with a view to model their dynamic behavior and especially to obtain detailed insights into the conformational coupling between the two rings. This paper is an additional example emphasizing the efficiency of a topological treatment for complex conformational situations.

On the basis of a formulation of the conformational coupling in terms of curvatures and bifurcations the first conclusion of this study is that the conformational processes of the two rings cannot be treated independently over the entire surface. As expected the largest barriers of these molecules are due to changes in the conformation of the six-membered ring. One-ring flip and two-ring flip mechanisms are nearly equally populated and both account adequately for the experimentally observed dependence of the barrier on heteroatom.

The other point of interest lies in a new strategy for deriving an effective potential surface of low dimension. The procedure involves the anihilation from the full hypersurface of adjacent critical points without altering the energetic characteristics of the interconversion network. The smoothed hypersurface becomes contractible to a three-dimensional effective one where the minimum of energetically lowest trajectories compatible with symmetry and experimental data lies.

Usual approaches using cross-sections or partial minimization could provide satisfactory energetical results too but not always with topological consistency. The present procedure overcomes the drawbacks inherent to the elimination a priori of some degrees of freedom (the lack of ascertained critical points). The pitfall of a bifurcating response during partial minimization is also avoided. Depending only on the connectivity between critical points and on an energetic tolerance, the smoothing procedure provides a useful tool for understanding and modeling complex systems in terms of low-dimensional effective potential hypersurface.

IV. Calculation Methods

Calculations were performed with our modified version of MM2,[4,7] including an original optimization package vectorized on a large scale for the implementation on a CRAY ONE system.

All optimizations were concluded with a few iterations of an appropriate NEWTON procedure.[24] They were considered converged when the root-mean-square value of the first derivative of the energy with respect to the coordinates was less than 5×10^{-8} kcal·mol^{-1}·Å^{-1}. Accuracy on the eigenvalues of the matrix of second derivatives was calculated to be better than one percent.

The Van der Waals parameters for oxygen and sulfur atoms were those proposed by ALLINGER: a spherical representation was adopted for sulfur[25] whereas lone pairs of electrons were explicitly taken into account in the description of the oxygen atom.[26] No treatment of "the anomeric effect" was included.[21a,27] A possible dependence of the barrier height on the solvent was not allowed for. Electrostatic interactions were omitted when the bond dipoles end at the same atom.

Appendix

Structure Labeling and Symmetry Considerations. Each conformation of free rings A and B of molecules **1** or **2** can be regarded as a distortion of a reference structure with C_{2v} symmetry. Generative nonrigid symmetry elements can be chosen as the following:

(a) The plane spanned by atoms 1, 4, 5 (Figure 1): A reflection across this plane induces a permutation-inversion of the torsional angles of ring A (e.g., C_6–C_7 dihedral becomes minus C_9–C_{10}) and inverts the signs of the torsional angles of ring B. This

(24) Liotard, D. *Thesis*, *Pau*, 1979.
(25) Allinger, N. L.; Hickey, M. J. *J. Am. Chem. Soc.* **1975**, *97*, 5167.
(26) Allinger, N. L.; Chang, S. H. M.; Glaser, D. H.; Honig, H. *Isr. J. Chem.* **1980**, *20*, 51.
(27) Jeffrey, G. A.; Taylor, R. *J. Comput. Chem.* **1980**, *1*, 99.

operation is designated with the symbol "*".

(b) The plane spanned by atoms 5, 6, 10 (perpendicular to the previous one): The corresponding symmetry operation is denoted with "—". It inverts ring A and inverts and permutates ring B.

These symmetry operations are commutative and both self invert ("**" = " "). C_1 conformations appear 4 times, C_2 or C_s conformations appear twice, and the central C_{2v} conformations are unique.

The nomenclature used for depicting the conformations of the cyclohexane ring is that proposed by Hendrikson[15a,b,c] for "chair" (C), "twist-boat" (TB), "boat" (B), and "planar" (P) and Anderson[1e] for "half-chair" (HC) and "half-boat" (HB). For five-membered rings one generally adheres to the distinction between half-chair (HC) and envelope (E) conformations.[5] However, spiro substitution may be the cause of severe distortions in ring B and the selected label can be somewhat conventional. In conformational sequences such as HC2b the capital letters refer to the conformation of ring A, the number 2 differentiates the nonsymmetrically related members of a given conformational family (Figure 2), and the small letter labels the conformation of ring B (Figure 3). The previously defined symmetry operations act on the parent label to give the equivalent labels (e.g., HC2*b*, HC2b, HC2*b*).

These notations allow a rapid identification of symmetrically equivalent structures without a detailed analysis of the torsional angles. The symmetry properties of free rings A and B propagate into the labels of **1** or **2**. For example, using the equal symbol for identical (not equivalent) conformations, C = C*, a = a* and therefore "—" acts on Ca to give Ca*. Similarly, TB1 = TB1* and the conformation TB1*a is invariant under the operation "*".

Acknowledgment. We express our gratitude to Professor E. Osawa (Hokkaido University, Sapporo, Japan) for allowing us to use his MM2 version. Our thanks are also due to Professor J. P. Penot (Université de Pau et des Pays de l'Adour, France) for helpful discussions about the mathematical aspects of the problem. This research was sponsored by the Centre de Calcul Vectoriel pour la Recherche, Ecole Polytechnique, Palaiseau (France), which is gratefully acknowledged.

Supplementary Material Available: Tables including the labeling matrix for **1** and torsional features, energies, and indices for nonsymmetrically related critical points of **1** and **2** and Figures 7 and 8 showing experimental and computed bandshapes of the *gem*-dimethyl group of **1** and **2** at different temperatures (7 pages). Ordering information is given on any current masthead page.

MBPT and Coupled-Cluster Investigation of Isomerization Reactions: $HCN \Longleftrightarrow HNC$, $BH_3CN^- \Longleftrightarrow BH_3NC^-$, and $HCNBH_3 \Longleftrightarrow HNCBH_3$

Miroslav Urban[†] and Rodney J. Bartlett*[,‡]

Contribution from the Quantum Theory Project, University of Florida, Gainesville, Florida 32611. *Received May 26, 1987*

Abstract: Heats of isomerization of title processes and binding energies of BH_3 to HCN, HNC, and CN^- were investigated by the fourth-order many-body perturbation theory (MBPT(4)) and coupled-cluster methods. Correlation effects are essential in the quantitative calculation of reaction heats of isomerization for H(CN) and $H(CN)BH_3$ and in binding energies of BH_3 toward HCN and HNC. Correlation effects are less important in reactions with the CN^- anion. Calculated isomerization energies are 64, 42, and 9 kJ/mol for H(CN), $BH_3(CN^-)$, and $H(CN)BH_3$ isomerizations, respectively. The binding energies of BH_3 to HCN and HNC are 71 and 124 kJ/mol, respectively, and the binding energies of BH_3 to CN^- and NC^- are 250 and 209 kJ/mol, respectively. Geometries of $H(CH)BH_3$ and $BH_3(CN)^-$ isomers were determined by a combination of MBPT(4) and gradient SCF methods.

Organoborates are interesting and important starting compounds in modern synthetic organic chemistry.[1] They are involved in reactions where migration of an organic group (or hydrogen) from boron to the acceptor carbon atom is usually exploited. An exceptional synthetic potential exists for cyanoborates,[2a] which may be regarded as donor–acceptor complexes of organoborane with HCN or HNC. The simplest compound of this type is $HCNBH_3$ and its isocyano isomer $HNCBH_3$. Since cyanoborate processes are usually initiated in salts,[2] BH_3CN^- and BH_3NC^- are of interest as well. In addition, since HNC is not normally available, BH_3CN^- and its subsequent protonated form contribute the source of the synthetically important $HNCBH_3$ molecule.[2]

In general, binding energies of molecules having weak dative bonds have been difficult to ascertain experimentally. This is particularly true for complexes of the transient monoborane species, BH_3, whose very short lifetime does not permit the direct determination of its energy. Although the binding energies of some related compounds, as e.g. BH_3CO, BH_3BH_3, and BH_3NH_3, have been investigated thoroughly both experimentally and theoretically (for a review, see ref 3a), little is known[4-6] about the geometry and the binding energy of HCN (and HNC) to BH_3. Particularly, we found no experimental data on binding energies of BH_3 to HCN, HNC, and CN^-, although all these BH_3 complexes were synthesized in the laboratory.[2] Recent semiempirical[4,5] and ab

[†] Present address: Department of Physical Chemistry, Faculty of Science, Comenius University, Mlynská dolina, 842 15 Bratislava, Czechoslovakia.
[‡] Guggenheim Fellow.

(1) Köster, Z. "Organobor-Verbindungen". *Methoden der Organischen Chemie (Houben-Weil)*; G. Thieme Verlag: Stuttgart, 1984; Vol. 13/3c.
(2) (a) Pelter, A.; Smith, K.; Hutchins, M. G.; Rowe, K. *J. Chem. Soc., Perkin Trans.* **1975**, 129. Pelter, A.; Hutchins, M. G.; Smith, K. *J. Chem. Soc. Perkin Trans 1* **1975**, 142. (b) Wade, R. C.; Sullivan, E. A.; Berschied, J. R.; Purcell, K. F. *Inorg. Chem.* **1970**, *9*, 2146.
(3) (a) Redmon, L. T.; Purvis, G. D., III; Bartlett, R. J. *J. Am. Chem. Soc.* **1979**, *101*, 2856. (b) Stanton, J.; Bartlett, R. J.; Lipscomb, W. N.; *Chem. Phys. Lett.* **1987**, *138*, 525. (c) Pople, J. A. *Faraday Discuss. Chem. Soc.* **1982**, *73*, 7.
(4) (a) Chadha, R.; Ray, N. K. *J. Indian Chem. Soc.* **1982**, *59*, 204. (b) Ray, N. K.; Chadha, R. *Theor. Chim. Acta* **1982**, *60*, 451.
(5) Bentley, T. W. *J. Org. Chem.* **1982**, *47*, 60.
(6) Marynick, D. S.; Throckmorton, L.; Bacquet, R. *J. Am. Chem. Soc.* **1982**, *104*, 1.

0002-7863/88/1510-4926$01.50/0